**PRELIMINARY MODELING OF THE IMPACT-INDUCED HYDROTHERMAL SYSTEM AT THE HAUGHTON IMPACT STRUCTURE.** A. J. Trowbridge[1], Simone Marchi[1], and Gordon R. Osinski[2], [1]Southwest Research Institute, Boulder, CO (alex.trowbridge@contractor.swri.org), [2]Dept. Earth Sciences, University of Western Ontario, London, ON, Canada.

**Introduction:** Subaereal and marine hydrothermal systems have been suggested to be important environments for prebiotic chemistry on early Earth [e.g. 1]. The high temperatures generated by hypervelocity impact has been shown to induce hydrothermal systems on Earth [2–4], as well as been proposed for Mars [5]. On Earth, post-impact induced hydrothermal systems (PIHs) are centers of localized fluid alteration and prebiotic chemistry [6], as exemplified by the Haughton impact structure, Canada [1, 7-9]. It is the purpose of this work to improve upon previous impact-induced hydrothermal modeling [e.g. 10-12] by fully coupling a hydrocode (iSALE) and a hydrothermal code (HYDROTHERM) to model the full evolution of impact-induced hydrothermal systems. Our aim is to validate our method by modeling the Haughton structure, before moving to Martian craters. Here, we present our preliminary results of Haughton crater.

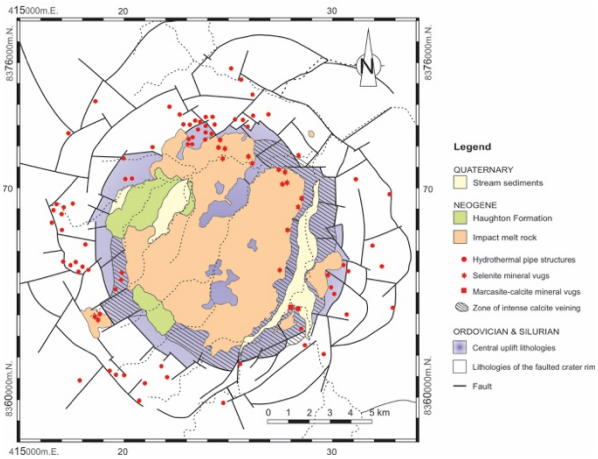


Figure 1. Simplified geological map of the Haughton structure. Modified from [13].

**Haughton Observational Constraints:** Haughton is a complex crater located on Devon Island, Nunavut, Northern Canada, see Figure 1 [13]. While the concentric normal faults give an apparent crater diameter of ~23 km, the proposed original crater rim diameter is actually ~16 km [13]. The material composing the central 8-9 km diameter of the crater floor is predominantly allochthonous crater-fill impactites composed of impact melt rock derived from 700 m to 2 km depth in the target stratigraphy, plus km-size uplifted blocks of Eleanor Rover Formation [13]. The crystalline basement, with a pre-impact depth of 1.9 km, is not exposed in the central uplift but is present as clasts in the crater-fill deposits [13]. At ~3.2-4 km radial distance to the east of the crater center, the Haughton river has exposed the upturned Bay Fiord Formation, which is derived from ~1000 m depth [13]. Further radially outward but still within the rim diameter, proximal ejecta can be found derived from 200 m to 1300 m [13]. The ballistic ejecta found outside the crater rim is derived from a depth of less than ~750 m [13]. We will use all of these observations to constrain our best-fit hydrocode impact model.

Evidence of PIH alteration at Haughton is predominately localized to five distinct regions [14]: (1) marcasite and calcite mineralization within crater-fill impact melt rocks; (2) the central uplift structure is cemented by hydrothermal quartz; (3) pervasive calcite veining around the edge of the central uplift; (4) hydrothermal pipe structures around the faulted crater rim; and (5) alteration of the ejecta. A proper hydrothermal model should contain all of these distinct regions within it; therefore, these are the constraints used in our hydrothermal model.

**Modeling Approach:** To model the vastly different timescales and physics of the crater-forming process and the PIHS, we used two separate codes (iSALE and HYDROTHERM) to model the full evolution of an impact-induced hydrothermal system.

*iSALE:* We used the iSALE shock physics code [15-17] for the hydrocode modeling. The runs were conducted in axisymmetric 2D. While this assumes a statistically unlikely vertical impact angle, we can account for this limitation by utilizing only the vertical component of the impact velocity ($v_i$), i.e. $v_i \cdot \sin(45^o)$ [18]. Our mesh geometry included a high-resolution zone containing cells of 16.25 m and extended 600 cells from the basin center and to a depth of 600 cells.

Due to current equations of state (EOS) limitation, the ~1.9 km of sedimentary rocks – which comprises ~75% carbonates (limestone and dolomite) with minor sandstones and shale – was modeled with the calcite ANEOS EOS [19], while the underlying granite bedrock and impactor were modeled with the granite and dunite ANEOS EOS, respectively [20, 21]. The anhydrite and gypsum-rich Bay Fiord Formation was also modeled with the calcite ANEOS EOS; however, it was given lesser strength to account for it being structurally weaker.

To simulate the rheology of the dunite, limestone, gypsum, and granite, we incorporated a rock-like strength model [16], a damage model with an exponential dependence on plastic strain [22], a dilatancy model [23], a thermal weakening model [24] corresponding to the temperature- and pressure-dependence of the material, and an acoustic fluidization model [25].

We conducted a parameter sweep of runs varying the projectile diameter, impactor velocity, and acoustic fluidization parameters until we matched the observational constraints discussed above.

*HYDROTHERM:* The hydrothermal modeling utilized the USGS code HYDROTHERM [26] version 3.2, which has been successfully used to model PIH systems by previous groups [10-12]. Unlike previous workers, we utilize the direct temperature, porosity, topography, and material layering from iSALE as the initial condition of our

HYDROTHERM runs. This is achieved by keeping the mesh geometry the same between the high-res zone of iSALE and HYDROTHERM (i.e. axisymmetric, 600 cells by 600 cells).

We assume a fixed value boundary condition at the surface with atmospheric pressure and temperatures, 1 bar and 20 ºC. Our current models contain a simplified permeability structure with a uniform permeability for each material type. This will change as our modeling becomes more developed. We run the simulations until the high temperatures after impact cool to the background thermal gradient.

**Results:** *iSALE:* Our best-fit model utilizes a 715 m in diameter dunite projectile with an impact velocity of 14 km/s (i.e. kinetic energy of ~$6.22 \cdot 10^{19}$ J). Figure 2 shows a plot of the Lagrangian tracer particles for this particular run. The tracer particles are color-coded to their origin depths with the black solid lines indicating material boundaries. It is apparent from this figure that we are matching the major observation constraints discussed above: none of the ballistic ejecta is sourced from depths greater than 750 m, the gypsum/Bay Fiord Formation is at the proper radial location ~3.2-4 km, the crater rim is ~16 km in diameter, and the central 8 km is derived from 700 m to 2 km depth in the target sequence.

For higher kinetic energies (higher impactor diameter or velocities), the ballistic ejecta begins to excavate deeper than 750 m. Similarly, we were not able to match the impactor rim diameter for smaller impact velocities.

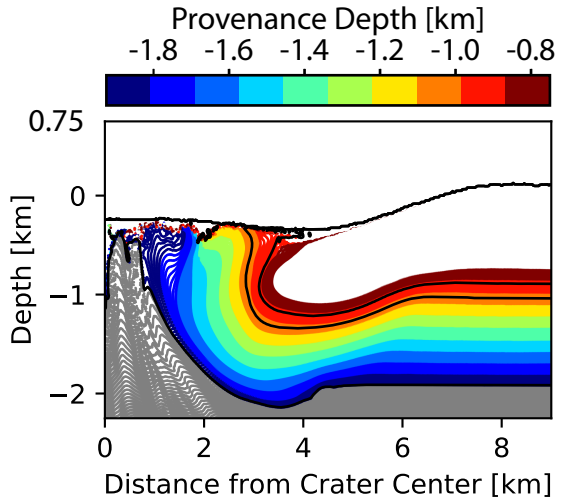


***Figure 2****: Lagrangian tracer particles for best-fit iSALE result. Note: black lines indicate material boundaries, the color of tracer particles > -750 m is fixed to white and < -1.9 km color is fixed to gray.*

*HYDROTHERM:* We have successfully coupled iSALE and HYDROTHERM, which has not been done by any previous studies into modeling PIHs [e.g. 10-12]. So far, our HYDROTERM models have been conducted for only simplified complex craters modeled with iSALE. From these preliminary runs, we are seeing concentrated alteration within the central crater and the edge of the central uplift, like observed in Haughton.

Additionally, we have observed that the lifetime of the hydrothermal system can be extended if there is an uplift of a less permeable underlying bedrock, like the granitic bedrock at Haughton. This is due to the concentrated fluid flow in the overlying more permeable layer, which decreases the cooling timescale of the post-impact temperatures. In contrast, the uplifted less permeable bedrock has less fluid flow, cools more conductively, and allows a transfer of higher temperatures to the overlying hydrothermal system; thereby, increasing the lifetime of the PIHs.

**Conclusions:** Our best-fit iSALE model utilizes a 715 m in diameter dunite projectile with an impact velocity of 14 km/s (i.e. kinetic energy of ~$6.22 \cdot 10^{19}$ J). We have successfully coupled iSALE and HYDROTHERM.. Our preliminary and simplified HYDROTHERM models illustrate the necessity to constrain PIHs modeling with accurate outputs from hydrocodes. Moving forward, we are planning to improve HYDROTHERM modeling to better represent our Haughton iSALE models; this includes the incorporation of depth and temperature dependent permeabilities as well as approximate fault locations with zones of high permeability.

**Acknowledgments:** We gratefully acknowledge the developers of iSALE-2D. Alex Trowbridge's research was supported by an appointment to the NASA Postdoctoral Program from the NASA Astrobiology Program at Southwest Research Institute administered by Oak Ridge Associated Universities under contract with NASA.

**References:** [1] Shulte, M., & Shock, E. L. (1995). *Orig. Life Evol. Biosphere* 25, 161-173. [2] Osinski, G.R., et al. (2001). *Meteorit. Planet. Sci.* 36, 731-745. [3] Koeberl, C., & Anderson, R.R. (1996). *G. S. of A.* 302. [4] Ames, D.E., et al. (1998). *Geology* 26, 447–450. [5] Newsom, H.E. (1980). *Icarus* 44, 207–216. [6] Osinski G. R., et al. (2020), *Astrobio.* 20, 1121–1149. [7] Voglesonger, K.M., et al. (1999). *Geol. Soc. Am. Abst. with Programs* 31, 488. [8] Farmer, J. (2000) *GSA today* 10, 1–9. [9] Brack, A. (2006). *Dev. Clay Sci.* 1, 379-391. [10] Rathbun, J.A., & Squyres, S.W. (2002). *Icarus* 157, 362-372. [11] Abramov, O., & Kring, D.A. (2005). *J. Geophys. Res.: Planets* 110. [12] Barnhart, C.J., et al. (2010). *Icarus* 208, 101-117. [13] Osinski, G.R., & Lee, P., (2005). *Meteorit. Planet. Sci.* 40, 1887–1900. [14] Osinski, G.R., et al. (2013). *Icarus* 224, 347-363. [15] Amsden, A., et al. (1980) *LANL Report*, 8095, 101p. [16] Collins, G.S., et al. (2004) *Meteoritics and Planet. Sci.*, 39, 217-231. [17] Wünnemann, K., et al. (2006) *Icarus*, 180, 514-27. [18] Johnson, B.C., et al. (2021). Icarus 366, 114539. [19] Pierazzo, E., et al. (1998). *J. Geophys. Res.* 103, 28607–28625. [20] Pierazzo, E., et al. (1997). *Icarus* 127, 408–423. [21] Pierazzo, E., et al. (2005). *Large meteorite impacts III* 384, 443-457. [22] Johnson, B.C., et al. (2016) *Science*, 354, 441-444. [23] Collins, G.S. (2014), *J. Geophys. Res. Planets*, 119, 2600–2619. [24] Ohnaka, M. (1995) *GRL*, 22, 25-28. [25] Wünnemann, K., & Ivanov., B.A. (2003). *Planet. Space Sci.* 51, 831–845. [26] Hayba, D.O., & Ingebritsen, S.E. (1994). *U.S. Geol. Surv. Water Resour. Invest. Rep.*